

Sub-Microscale Speckle Pattern Creation on Single Carbon Fibers for In-Situ DIC Experiments

KARAN SHAH, GENE YANG, MOHAMMAD EL LOUBANI,
SUBRAMANI SOCKALINGAM and DONGKYU LEE

ABSTRACT

High performance carbon and glass fibers are widely used as reinforcements in composite material systems for aerospace, automotive, and defense applications. Modifications to fiber surface treatment (sizing) is one of the ways to improve the strength of fibers and hence the overall longitudinal tensile strength of the composite. Single fiber tensile tests at the millimeter scale are typically used to characterize the effect of sizing on fiber strength. However, the characteristic length-scale governing the composite failure due to a cluster of fiber breaks is in the micro-scales. To access such micro-scale gage-lengths, we aim to employ indenters of varying radii to transversely load fibers and use scanning electron microscope (SEM) with digital image correlation (DIC) to measure strains at these length-scales. The use of DIC technique requires creation of a uniform, random, and high contrast speckle pattern on the fiber surface such as that shown in Figure 1. In this work, we investigate the formation of sub-microscale speckle pattern on carbon fiber surface via sputter deposition and pulsed laser deposition techniques (PLD) using Gold-Palladium (Au-Pd) and Niobium-doped SrTiO₃ (Nb:STO) targets respectively. Different processing conditions are investigated for both sputter deposition: sputtering current and coating duration, and PLD: number of pulses respectively to create sub-micron scale patterns viable for micro-DIC on both sized and unsized carbon fibers. By varying the deposition conditions and SEM-imaging the deposited patterns on fibers, successful pattern formation at sub-micron scale is demonstrated for both as-received sized and unsized IM7 carbon fibers of average diameter 5.2 μm via sputter deposition and PLD respectively.

INTRODUCTION

High performance carbon fibers are widely used as fiber reinforcements in composite material systems for aerospace, automotive, and defense applications. The longitudinal tensile failure of such composite systems is known to occur as a series of single fiber breaks, progressing into a cluster of 'N' fiber breaks and eventually leading to failure of the composite once the critical cluster size of N^* fiber breaks is reached [1,2]. The axial distance between these cluster of fiber breaks is observed to be between less than one fiber radius [2] ($3.5 \mu\text{m}$ for the carbon fiber) and one ineffective length, ' δ ', of the fiber [3] suggesting that the strength of the composite is controlled by flaws active at those length-scales. It is thus important to measure the tensile strength distribution of fibers at these micro-scale lengths in order to assess the influence of sizing. However, it is challenging to characterize the strength distribution of fiber at such micro-scales. Traditional single fiber tensile testing method is not applicable because it is limited by the smallest gage-length that can be tested via this method due to clamp effects in testing [4]. Past work in the area of determining single fiber strength distribution at micro-scale gage-lengths involve the use of single fiber fragmentation tests [5], loop tests [6], and notch tests [7,8]. Although, loop tests and notch test methods allow access to much smaller gage-lengths owing to the stress localization around the notch and the loop, the strength distributions determined from these tests is subject to the parameters such as elastic constants used in the calculation. Besides, local measurement of the stresses or strain concentration in fibers around the loop or notch was not performed in the studies mentioned above.

In our study, we aim to employ digital image correlation using scanning electron microscope (SEM-DIC technique) [9,10] to measure stress/strain concentrations developed in carbon fibers at the characteristic micro-scales associated with composite failure. The micro-scale lengths will be accessed using a quasi-static transverse loading experimental set-up that is generally employed to study the failure behavior of ballistic fibers under transverse loading with different indenter geometries. Modeling of such experiments for Kevlar® [11] and Dyneema® [12] single fibers under transverse loading from a fragment simulating projectile FSP ($R = 20 \mu\text{m}$) and razor blade ($R \sim 2 \mu\text{m}$) has shown that stress concentrations at the fiber-indenter contact zone occur over lengths on the order of the indenter tip radius. Thus, we aim to employ the said transverse loading method to access the micro-scale gage-lengths in carbon fibers via different indenter geometries having tip radii to induce stress concentrations over lengths on the order of the characteristic length-scales observed in composite failure.

However, the use of SEM-DIC technique requires a uniform, random, and highly contrastive speckle pattern on the fiber surface with speckle or feature sizes at sub-micron scale resolution. Kammers and Daly [13] have reported a review of patterning methods at nanometer length-scales which involves methods such as chemical vapor thin film arrangement, template patterning, nanoparticle patterning, focused ion beam patterning, and e-beam lithography. However, all the methods discussed in their study are either time consuming, expensive, or damaging to the fiber specimen and or involve a multi-step process including some surface treatment of the specimen to allow patterns to be created. For the purposes of this study, we intend to generate a pattern on the fiber surface in its as-is condition

without a) chemically modifying the fiber surface to make it viable for pattern generation, and b) damaging the fiber surface during deposition. In addition, the method for pattern creation must be simple and efficient to perform with as few steps as possible owing to the difficulty in handling single fiber specimens.

Hence, we utilize physical vapor deposition techniques like sputter deposition and pulsed laser deposition (PLD) techniques to investigate the creation of sub-micron scale speckle pattern on single fibers. In a recent study, Hoefnagels et al. [14] has shown the use of sputter deposition technique to create nano-micron scale speckle patterns of InSn alloy on silicon, polyimide, and pure FE substrates for in-situ micromechanical testing. PLD technique has also been used to form metal nanoparticles on a variety of substrates such as silicon [15,16], sapphire [15], glass [16,17], and CaF₂ [17] substrates. The PLD technique also offer some advantages over the sputter deposition technique in terms of better control over the size, dimension, and distribution of metal nanoparticles [18]. Since both these methods were shown to work on different substrates, in this study we explore these techniques for pattern creation on single carbon fibers. To the authors' knowledge, such an investigation of pattern creation on single fibers for micro-DIC application has not been published before. Pattern creation on both sized and unsized carbon fibers will be considered in this study as fiber sizing is also known to have influence on the tensile and interfacial shear strength of the composite [19].

METHODS

Sized and Unsized IM7 carbon fibers were acquired in the form of a spool from Hexcel Corporation. The sized IM7 fiber had a proprietary 'GP' sizing as specified by Hexcel which is compatible with epoxy, phenolic, vinyl ester, polyurethane, and cyanate ester-based matrices and had an average diameter of 5.2 μm as specified in the Hexcel datasheet. The unsized IM7 fiber had an average diameter of approximately 5.08 μm as measured from our SEM images. A Zeiss FE500 SEM with a secondary electron detector was used to capture all the images taken in this study.

Sputter Deposition

A Denton Vacuum Desk II sputter coater was used with a gold-palladium target (Au-Pd) to investigate the generation of speckle pattern on single carbon fibers via sputter coating. The pattern created via sputtering is known to depend on deposition conditions including temperature, sputter current, chamber pressure, duration of coating and on the target and the substrate material used [20]. For a metal alloy target of In-Sn alloy, Hoefnagels et al. [14] reported that higher currents and deposition times lead to larger features (speckles) whereas higher chamber pressures resulted in smaller features. The feature size is understood to be mainly governed by adatom (atoms adsorbed on the surface) mobility, which is higher at lower pressure surface due to fewer collisions of the target atoms with the background gas [21]. Thus, at lower pressures more target atoms are able to reach the substrate surface leading to larger features. However, all sputter deposition in this study was carried out at a pressure between ~120-140 mTorr as it is difficult to

achieve lower pressures using the Denton Vacuum sputter coater without a turbo pump. Additionally, all sputter deposition was performed at room temperature to minimize any alterations in the fiber properties due to an increase in temperature. In this study, the deposition conditions varied for sputter deposition were sputter current and sputter duration. Table 1 presents the different current conditions and duration of sputtering investigated for the sized and unsized IM7 fiber. The sputter coated fibers were then imaged inside a Zeiss Gemini FE500 SEM to study the effect of sputtering conditions on surface deposition and pattern creation.

Table 1. Sputtering conditions investigated for IM7 carbon fiber.

Fiber	Target	Current (mA)	Pressure (mTorr)	Duration (mins)
Sized IM7 fiber	Au-Pd	50	~120-140	3
Sized IM7 fiber	Au-Pd	40	~120-140	5
Sized IM7 fiber	Au-Pd	40	~120-140	10
Sized IM7 fiber	Au-Pd	50	~120-140	5
Sized IM7 fiber	Au-Pd	50	~120-140	10
Unsized IM7 fiber	Au-Pd	50	~120-140	5
Unsized IM7 fiber	Au-Pd	50	~120-140	10

Pulsed Laser Deposition

A KrF excimer laser was used at $\lambda = 248$ nm, 10 Hz pulse rate, and 1 J/cm^2 pulse energy. A niobium doped strontium titanate (Nb:STO) was coated as this material is widely used for obtaining high conductivity among various metal oxides [22]. Generally, the deposition by PLD is mainly dependent on temperature and background pressure during the deposition of materials [23]. Carbon fibers are vulnerable to heat treatments [24], whereas the metal deposition process by PLD requires a thermal annealing process. Furthermore, the deposition of metals also needs to be done in certain gas ambient [23]. Therefore, we first tested a temperature of $150 \text{ }^\circ\text{C}$ and an oxygen partial pressure of ~ 100 mTorr to deposit metal oxides to assess if any speckle pattern is formed under these deposition conditions. In fact, for the formation of speckle patterns by PLD, the number of pulses seems to be more critical rather than temperature and background pressure [25]. Four deposition conditions with different number of pulses (7000, 8000, 9000, 12000) were performed on both sized and unsized carbon fibers to induce different types of speckle patterns. Finally, PLD coated carbon fibers were imaged under microscope and SEM (Zeiss Gemini FE500) to observe any generated speckle pattern.

RESULTS & DISCUSSION

The region of interest (ROI) for our in-situ SEM-DIC experiments is the area of stress-strain concentration developed under the fiber-indenter contact (example $4 \text{ } \mu\text{m}$ for razor blade). Thus, the field of view (FOV) chosen for SEM-DIC experiments must effectively capture this ROI and the ROI must contain a high

contrast speckle pattern with speckles of appropriate size to obtain accurate measurements of the underlying specimen deformation. DIC guidelines require that: a) the patterned features (speckle) must occupy an area of at least $3 \times 3 \text{ pixel}^2$ and b) each subset of size $M \times M$ within the region of interest (ROI) must contain at least 3×3 features or speckles to achieve accurate correlation [26]. Subsets are small virtual portions of the region of interest (ROI) which are compared when correlating images in the reference and deformed configuration in DIC analysis. For any given FOV, the feature or the speckle size determines the spatial resolution of the system that can be obtained. And as mentioned above, the speckle size also determines the minimum subset size required for accurate matching between subsets. There are many metrics available in the literature on the appropriate choice of subset size [27–29] for a particular application, however a detailed investigation into the appropriate choice of subset size and speckle pattern quality assessment is outside the scope of current study and is subject of future investigation. The patterns obtained on carbon fibers via sputter coating and PLD will be qualitatively discussed in the following sections considering the FOV and the DIC guidelines mentioned above.

Patterns created using Sputter Deposition

Figures 1-4 show the speckle pattern obtained for the sized and unsized IM7 carbon fibers for the sputtering conditions presented in Table 1. All the images presented in Figures 1-4 are shown at approximately similar FOVs to allow for comparisons to be made between the different patterns. As seen from Figure 1 for a sputter duration of 3 minutes, clusters of Au-Pd particles appear to be forming on the fiber surface. However, the clusters seem to still be in their development phase and its boundaries are not well-defined. In other words, the pattern deposited on the fiber surface does not have enough features with sufficient contrast to be applicable for DIC.

As the sputter duration is increased from 3 minutes to 5 minutes to 10 minutes, formation of a greater number of clusters is observed on the fiber surface as seen from Figures 2 and 3 for both sputtering currents of 40 mA and 50 mA, respectively. It can also be observed that increasing the sputtering current for the same duration of coating, results in clusters of particles with well-defined boundaries and hence greater contrast (bright speckles surrounded by dark region) on the fiber surface.

As per DIC guidelines, for a horizontal field width (HFW) of $4 \mu\text{m}$ and an image resolution of 1024 pixels, the minimum required speckle size is approximately 12 nm. For all the pattern images in Figures 2 and 3, it can be gleaned just by observation that the average speckle size is greater than this minimum requirement of 12 nm. Figures 2 and 3 also show two square grids overlaid on the patterns to denote two different subset sizes of $100 \times 100 \text{ pixel}^2$ (red grid) and $50 \times 50 \text{ pixel}^2$ (yellow grid). As seen from Figure 2(a), the pattern created using a sputter current of 40 mA and a duration of 5 minutes consists of larger clusters or speckles with poor contrast and a minimum subset size of $100 \times 100 \text{ pixels}^2$ is required to accommodate a minimum of 3 speckles. For the pattern generated using a current of 40 mA and duration of 10 minutes (Figure 2(b)), have cluster sizes that are relatively smaller than those in Figure 2(a) and have a better

contrast. The pattern, however, seems to contain a relatively higher proportion of larger clusters than smaller clusters and hence a larger subset size ($100 \times 100 \text{ pixel}^2$) may be required for better correlation. Pattern in Figure 3(a) for a sputter current of 50 mA and duration of 5 minutes has a better contrast than the pattern in Figure 2(a) for a sputter current of 40 mA, however, the cluster sizes are relatively large requiring the use of a larger subset size. By far the best contrast is obtained for pattern shown in Figure 3(b) for a sputter current of 50 mA and a duration of 10 minutes. This pattern also has a good distribution of different cluster sizes allowing for the use of a small subset size of $50 \times 50 \text{ pixel}^2$. For a given FOV, smaller subset sizes offer higher spatial resolution than larger subset sizes as required for measuring deformation in areas of stress concentration. For patterns with relatively larger speckles, it might be possible to use a larger FOV (lower magnification) and thereby use a smaller subset size for accurate matching. However, using a larger FOV also reduces the spatial resolution required in the ROI for a particular application. Thus, a larger average speckle size forces the use of larger subset size for a given FOV which can lead to incorrect approximation of underlying displacements [27]. Thus, out of all the patterns obtained, the pattern in Figure 3(b) is a good candidate for capturing the area of stress concentrations developed in fibers during transverse loading.

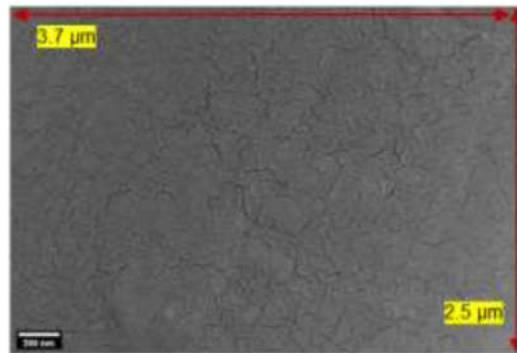
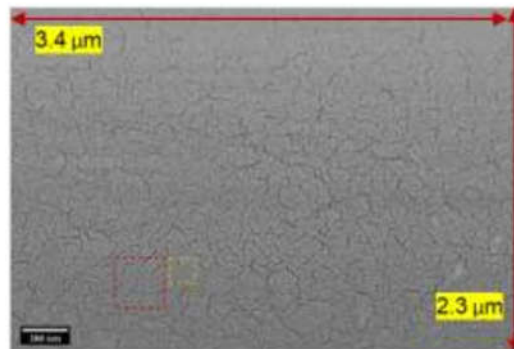
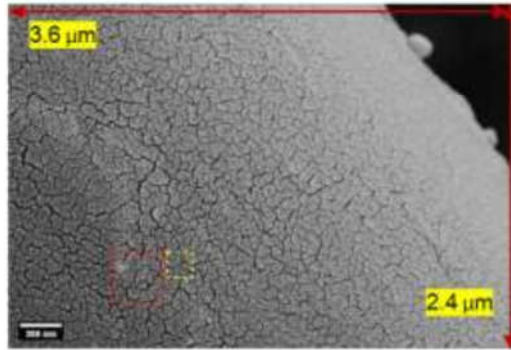


Figure 1. SEM image of sized IM7 fiber pattern using a sputter current of 50mA and a duration of 3 minutes.

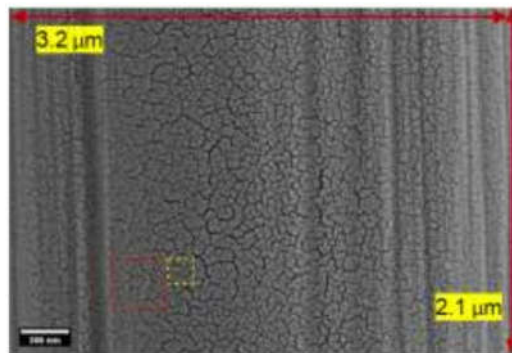


(a)

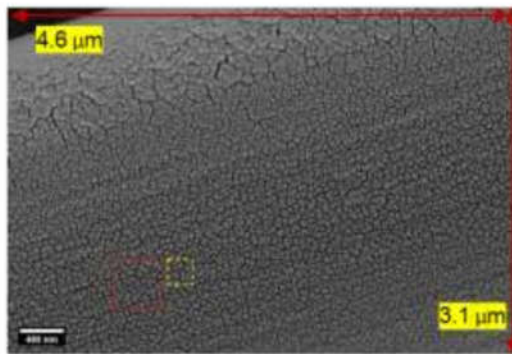


(b)

Figure 2. SEM images of sized IM7 carbon fiber for a sputtering current of 40 mA and sputter duration of a) 5 mins, and b) 10 mins.



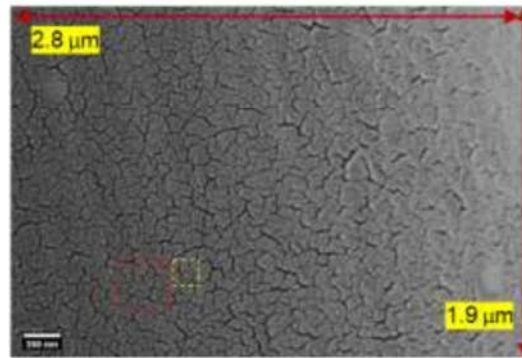
(a)



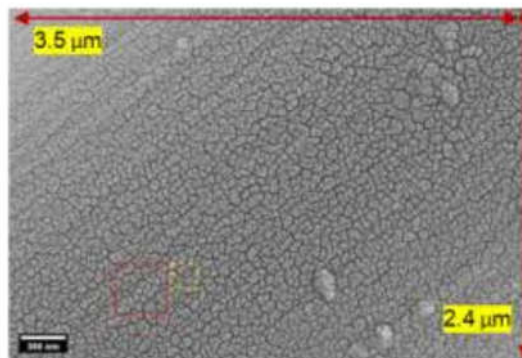
(b)

Figure 3. SEM images of sized IM7 carbon fiber taken at different magnifications for a sputtering current of 50 mA and sputter duration of a) 5 mins, and b) 10 mins.

Since a higher sputter current was shown to induce patterns with better contrasts, pattern formation on unsized IM7 fibers was investigated at a sputter current of 50 mA and sputter duration of 5 minutes and 10 minutes. Figure 4 shows the resulting patterns formed on the fiber surface. Similar patterns as that obtained for the sized IM7 fiber in Figure 3 are obtained for the unsized fiber. Again, sputtering conditions of 50 mA sputter current and duration of 10 minutes were shown to form a pattern on the fiber surface with good contrast and distribution of speckle sizes.



(a)



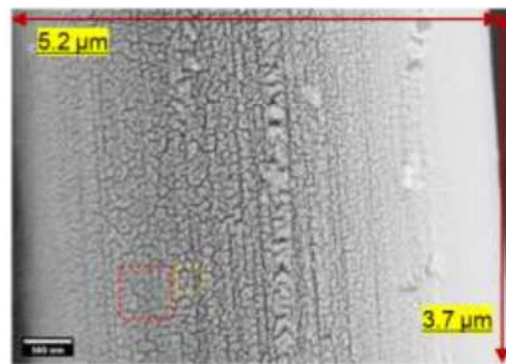
(b)

Figure 4. SEM images of unsized IM7 carbon fiber for a sputter current of 50 mA and sputter duration of a) 5 mins, and b) 10 mins.

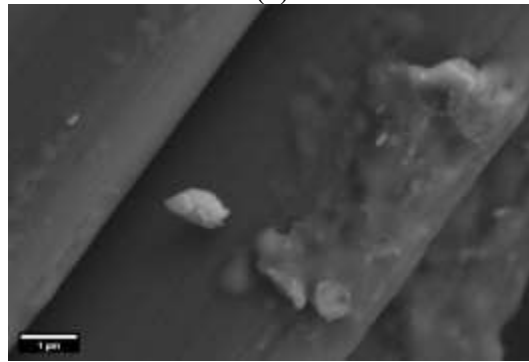
Patterns created using PLD

Figures 5 and 6 show the speckle patterns obtained on sized and unsized carbon fibers for different number of pulses used during PLD. Patterns with distinct speckles or features of Nb:STO particles were not observed for fewer than 7000 pulses, hence the images for those patterns are not reported here. For pulses greater than 12000, patterns were also not observed on the fiber surface for both sized and unsized as shown in Figures 5(b) and 6(b). This may be because of the agglomeration of particles at higher number of pulses of 12000. It was observed that the optimized number of pulses to obtain patterns was 8000 pulses for sized carbon fibers and 9000 pulses for unsized carbon fibers. The SEM images of sized carbon fibers at both 8000 and 12000 pulses are shown in Figure 5(a) and 5(b) respectively. Square grids of $50 \times 50 \text{ pixel}^2$ and $100 \times 100 \text{ pixel}^2$ are also overlaid on the images to denote two different subset sizes as previously shown for the sputter coated images. As seen from Figure 5(a), the pattern deposited on the sized fiber for 8000 pulses consists of speckles with good contrast (bright speckles surrounded by dark regions). The pattern also contains a good distribution of large and small speckle sizes and a smaller subset size of $50 \times 50 \text{ pixel}^2$ can be used with this pattern. As the number of pulses is increased to 12000, Nb:STO particles seems to agglomerate on a small region of fiber instead of forming patterns. This may be due to an increase in thickness of the deposited material as the number of pulses is increased to 12000. As more and more material is being deposited, the excess

material filled in the gap between the patterns and the clusters of Nb:STO particles agglomerate and hence the pattern disappeared and agglomeration occurred. For the unsized carbon fibers, Figure 6(a),(b) show the imaged carbon fibers for 9000 and 12000 pulses, respectively. Similar results as that observed for the sized carbon fibers were obtained for the unsized fibers. A pattern of Nb:STO pattern with good contrast was obtained at 9000 pulses (Figure 6(a)) whereas for 12000 pulses (Figure 6(b)), the deposited material seem to have agglomerated on top of each other, and no speckle pattern was observed. Compared to the sized fiber, the average speckle sizes seem to be slightly larger for unsized fibers coated with 9000 pulses and hence may require the use of slightly larger subset than $50 \times 50 \text{ pixel}^2$ as shown in Figure 6(a). A further investigation into pattern creation using different partial pressures and temperatures using PLD with Nb:STO target and other metal targets is part of a future study.

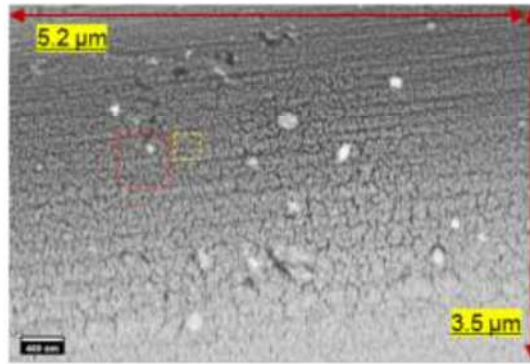


(a)

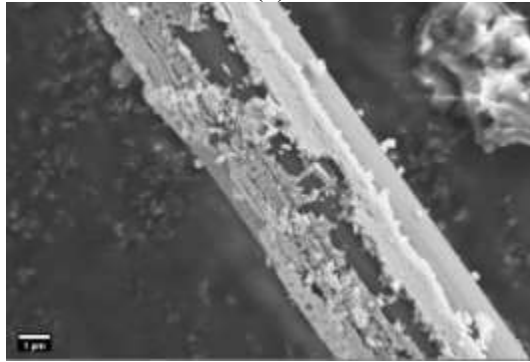


(b)

Figure 5. SEM images of sized carbon fibers using (a) 8000 pulses and (b) 12000 pulses.



(a)



(b)

Figure 6. SEM images of unsized carbon fibers using (a) 9000 pulses and (b) 12000 pulses.

CONCLUSIONS

This study investigated the pattern formation on sized and unsized IM7 fibers via physical vapor deposition techniques including sputter coating and pulsed laser deposition for in-situ micro-DIC experiments. Fibers were coated at various sputter coating (current and duration) and PLD (number of pulses) conditions to investigate the type of patterns formed on the fiber surface. For sputter coating with Au-Pd target, it was found that a higher current (50 mA) and a longer duration (10 mins) of coating results in a good distribution of speckle sizes on the fiber surface with better contrast and hence make good candidates for SEM-DIC analysis. For PLD, patterns with sufficient number of features and good contrast were observed at 8000 pulses and 9000 pulses for sized and unsized fibers respectively. Increasing the number of pulses to 12000 lead to particle agglomeration and pattern deterioration. Both methods of deposition have shown that it is possible to alter the type of pattern in terms of the size and distribution of features deposited on the fiber surface by varying the sputter coating or PLD conditions. In the future, we plan to investigate pattern formation at varying pressures for sputter coating and at varying pressures and temperature for PLD.

ACKNOWLEDGMENTS

This material is based upon work supported by the National Science Foundation under Grant No. CMMI-1915948. Any opinions, findings, and conclusions or recommendations expressed in this material are those of the author(s) and do not necessarily reflect the views of the National Science Foundation. Sized and unsized IM7 fibers used in this study provided by Hexcel corporation is gratefully acknowledged.

REFERENCES

- [1] Aroush DR Ben, Maire E, Gauthier C, Youssef S, Cloetens P, Wagner HD. A study of fracture of unidirectional composites using in situ high-resolution synchrotron X-ray microtomography. *Compos Sci Technol* 2006;66:1348–53. doi:10.1016/j.compscitech.2005.09.010.
- [2] Swolfs Y, Morton H, Scott AE, Gorbatiikh L, Reed PAS, Sinclair I, et al. Synchrotron radiation computed tomography for experimental validation of a tensile strength model for unidirectional fibre-reinforced composites. *Compos Part A Appl Sci Manuf* 2015;77:106–13. doi:10.1016/j.compositesa.2015.06.018.
- [3] Rosen-Tensile-failure-of-fibrous-comp-1964.pdf n.d.
- [4] Phoenix SL, Sexsmith RG. Clamp Effects in Fiber Testing. *J Compos Mater* 1972;6:322–37. doi:10.1177/002199837200600311.
- [5] Watanabe J, Tanaka F, Okuda H, Okabe T. Tensile strength distribution of carbon fibers at short gauge lengths. *Adv Compos Mater* 2014;23:535–50. doi:10.1080/09243046.2014.915120.
- [6] Okuda H, Young RJ, Tanaka F, Watanabe J, Okabe T. Tensile failure phenomena in carbon fibres. *Carbon N Y* 2016;107:474–81. doi:10.1016/j.carbon.2016.06.037.
- [7] Shioya M, Inoue H, Sugimoto Y. Reduction in tensile strength of polyacrylonitrile-based carbon fibers in liquids and its application to defect analysis. *Carbon N Y* 2013;65:63–70. doi:10.1016/j.carbon.2013.07.102.
- [8] Sugimoto Y, Shioya M, Kageyama K. Determination of intrinsic strength of carbon fibers. *Carbon N Y* 2016;100:208–13. doi:10.1016/j.carbon.2016.01.021.
- [9] Sutton MA, Li N, Joy DC, Reynolds AP, Li X. Scanning electron microscopy for quantitative small and large deformation measurements Part I: SEM imaging at magnifications from 200 to 10,000. *Exp Mech* 2007;47:775–87. doi:10.1007/s11340-007-9042-z.
- [10] Sutton MA, Li N, Garcia D, Cornille N, Orteu JJ, McNeill SR, et al. Scanning electron microscopy for quantitative small and large deformation measurements Part II: Experimental validation for magnifications from 200 to 10,000. *Exp Mech* 2007;47:789–804. doi:10.1007/s11340-007-9041-0.

- [11] Sockalingam S, Gillespie JW, Keefe M. Influence of multiaxial loading on the failure of Kevlar KM2 single fiber. *Text Res J* 2018;88:483–98. doi:10.1177/0040517516681961.
- [12] Sockalingam S, Thomas FD, Casem D, Gillespie JW, Weerasooriya T. Failure of Dyneema® SK76 single fiber under multiaxial transverse loading. *Text Res J* 2019;89:2659–73. doi:10.1177/0040517518798653.
- [13] Kammers AD, Daly S. Small-scale patterning methods for digital image correlation under scanning electron microscopy. *Meas Sci Technol* 2011;22. doi:10.1088/0957-0233/22/12/125501.
- [14] Hoefnagels JPM, van Maris MPFHL, Vermeij T. One-step deposition of nano-to-micron-scalable, high-quality digital image correlation patterns for high-strain in-situ multi-microscopy testing. *Strain* 2019;55:1–13. doi:10.1111/str.12330.
- [15] Donnelly T, Krishnamurthy S, Carney K, McEvoy N, Lunney JG. Pulsed laser deposition of nanoparticle films of Au. *Appl Surf Sci* 2007;254:1303–6. doi:10.1016/j.apsusc.2007.09.033.
- [16] Agarwal NR, Neri F, Trusso S, Lucotti A, Ossi PM. Au nanoparticle arrays produced by Pulsed Laser Deposition for Surface Enhanced Raman Spectroscopy. *Appl Surf Sci* 2012;258:9148–52. doi:10.1016/j.apsusc.2011.12.030.
- [17] Domingo C, Resta V, Sanchez-Cortes S, García-Ramos J V., Gonzalo J. Pulsed laser deposited au nanoparticles as substrates for surface-enhanced vibrational spectroscopy. *J Phys Chem C* 2007;111:8149–52. doi:10.1021/jp0710943.
- [18] Jing Y, Wang H, Chen X, Wang X, Wei H, Guo Z. Pulsed laser deposited Ag nanoparticles on nickel hydroxide nanosheet arrays for highly sensitive surface-enhanced Raman scattering spectroscopy. *Appl Surf Sci* 2014;316:66–71. doi:10.1016/j.apsusc.2014.07.169.
- [19] Zhang RL, Huang YD, Su D, Liu L, Tang YR. Influence of sizing molecular weight on the properties of carbon fibers and its composites. *Mater Des* 2012;34:649–54. doi:10.1016/j.matdes.2011.05.021.
- [20] Alfonso E, Olaya J, Cubillos G. Thin Film Growth Through Sputtering Technique and Its Applications. *Cryst - Sci Technol* 2012. doi:10.5772/35844.
- [21] Jung YS, Lee DW, Jeon DY. Influence of dc magnetron sputtering parameters on surface morphology of indium tin oxide thin films. *Appl Surf Sci* 2004;221:136–42. doi:10.1016/S0169-4332(03)00862-6.
- [22] Tomio T, Miki H, Tabata H, Kawai T, Kawai S. Control of electrical conductivity in laser deposited SrTiO₃ thin films with Nb doping. *J Appl Phys* 1994;76:5886–90. doi:10.1063/1.358404.
- [23] Morintale E, Constantinescu C, Dinescu M. Thin films development by

- pulsed laser-assisted deposition. *Ann Univ Craiova, Phys* 2010;20:43–56.
- [24] Li B, Zhang CR, Cao F, Wang SQ, Chen B, Li JS. Effects of fiber surface treatments on mechanical properties of T700 carbon fiber reinforced BN-Si₃N₄ composites. *Mater Sci Eng A* 2007;471:169–73. doi:10.1016/j.msea.2007.03.022.
- [25] Gonzalo J, Perea A, Babonneau D, Afonso CN, Beer N, Barnes JP, et al. Competing processes during the production of metal nanoparticles by pulsed laser deposition. *Phys Rev B - Condens Matter Mater Phys* 2005;71:1–8. doi:10.1103/PhysRevB.71.125420.
- [26] Schreier H, Orteu JJ, Sutton MA. Image correlation for shape, motion and deformation measurements: Basic concepts, theory and applications. 2009. doi:10.1007/978-0-387-78747-3.
- [27] Yaofeng S, Pang JHL. Study of optimal subset size in digital image correlation of speckle pattern images. *Opt Lasers Eng* 2007;45:967–74. doi:10.1016/j.optlaseng.2007.01.012.
- [28] Crammond G, Boyd SW, Dulieu-Barton JM. Speckle pattern quality assessment for digital image correlation. *Opt Lasers Eng* 2013;51:1368–78. doi:10.1016/j.optlaseng.2013.03.014.
- [29] Dong YL, Pan B. A Review of Speckle Pattern Fabrication and Assessment for Digital Image Correlation. *Exp Mech* 2017;57:1161–81. doi:10.1007/s11340-017-0283-1.